Food Chemistry: X 24 (2024) 101870

Contents lists available at ScienceDirect

Food Chemistry: X

journal homepage: www.sciencedirect.com/journal/food-chemistry-x

In vitro digestion and fecal fermentation behaviors of exopolysaccharide from *Morchella esculenta* and its impacts on hypoglycemic activity *via* PI3K/Akt signaling and gut microbiota modulation

Weihong Guo [a], Xuerui Wang [a], Biao Wang [a], Yajie Zhang [a], Fengyun Zhao [a], Yuling Qu [a], Liang Yao [b], Jianmin Yun [a,*]

[a] College of Food Science and Engineering, Gansu Agricultural University, Lanzhou 730070, Gansu, China
[b] Gannong Moli (Qingyang) Agricultural Development Co., Ltd, Qingyang 745000, Gansu, China

ARTICLE INFO

Keywords:
Morchella esculenta
Extracellular polysaccharides
Simulated gastrointestinal digestion
Fecal fermentation
Hypoglycemic activity

ABSTRACT

This study aimed to evaluate the effects of gastrointestinal digestion on the physicochemical properties and hypoglycemic activity of extracellular polysaccharides from *Morchella esculenta* (MEPS). The results showed that the MEPS digestibility was 22.57 % after saliva-gastrointestinal digestion and only partial degradation had occurred. Contrarily, after 48 h of fecal fermentation, its molecular weight and molar ratios of the monosaccharide composition varied significantly due to being utilized by human gut microbiota, and the final fermentation rate was 76.89 %. Furthermore, the MEPS-I, the final product of saliva-gastrointestinal digestion still retained significant hypoglycemic activity, it alleviated insulin resistance and increased the IR cells glucose consumption by activating PI3K/AKT signaling pathway. MEPS-I treatment reduced the proportion of *Firmicutes* to *Bacteroidetes*, and the relative abundance of beneficial bacteria that enhanced insulin sensitivity and glucose uptake was promoted. This research can provide a theoretical basis for the further development of *Morchella esculenta* as a health functional food.

1. Introduction

Edible fungi have gradually become an important part of people's daily diet due to their rich nutrients and significant medicinal properties (Zhang et al., 2021). Recently, a large number of researchers have extracted, characterized and analyzed the bioactive components in various edible fungi, such as polysaccharides, peptides and phenols (Wang, Wang, Xu, & Ding, 2017). Among them, polysaccharides have attracted much attention due to their great therapeutic potential and have been proven to possess a variety of biological activities such as immunoregulation, anti-tumor and hypoglycemic properties (Ma et al., 2022). Polysaccharides from edible fungi are generally divided into fruiting polysaccharides, as well as intracellular and extracellular polysaccharides by submerged fermentation. There are some differences in chemical structure and active functions of polysaccharides from different sources (Wu et al., 2023).

As a complex metabolic disease, diabetes mellitus (DM) is characterized by abnormal insulin metabolism, hyperglycemia and dyslipidemia, and is accompanied by some complications (Wang et al., 2017). Insulin is a pivotal hormone in the regulation of blood glucose, but insulin resistance hinders insulin's function of maintaining glucose and lipid homeostasis, which is closely associated with all stages of DM, including prediabetes, diabetes and its complications (Khalid, Alkaabi, Khan, & Adem, 2021; Zhao et al., 2023). Due to the side effects of various oral drugs used to treat diabetes, researchers have focused the development of drugs to improve IR and lower blood glucose using natural active ingredients with lower side effects (Xu, Li, Dai, & Peng, 2018). Studies found that biologically active polysaccharides from edible mushrooms could effectively prevent and control the development of diabetes and its complications by inhibiting cell oxidative stress, alleviating IR, regulating glucose and glycogen metabolism (Cai et al., 2020; Liu et al., 2020; Xiang, Sun-Waterhouse, & Cui, 2021). Research has also shown that polysaccharides from *Ganoderma lucidum*, *Cordyceps militaris*, *Lentinula edodes* and *Poria cocos* can alleviate and improve diabetes by regulating gut microbiota (Yu, Luo, Liu, & Peng, 2023).

Generally, the bioavailability of polysaccharides depends not only on their physicochemical properties and structural characteristics, but also on their absorption and utilization by the human digestive system.

* Corresponding author at: College of Food Science and Engineering, Gansu Agricultural University, No. 1 Yingmencun, Anning District, Lanzhou 730070, China.
E-mail address: yunjianmin@gsau.edu.cn (J. Yun).

https://doi.org/10.1016/j.fochx.2024.101870
Received 26 August 2024; Received in revised form 28 September 2024; Accepted 30 September 2024
Available online 2 October 2024
2590-1575/© 2024 The Authors. Published by Elsevier Ltd. This is an open access article under the CC BY-NC-ND license (http://creativecommons.org/licenses/by-nc-nd/4.0/).

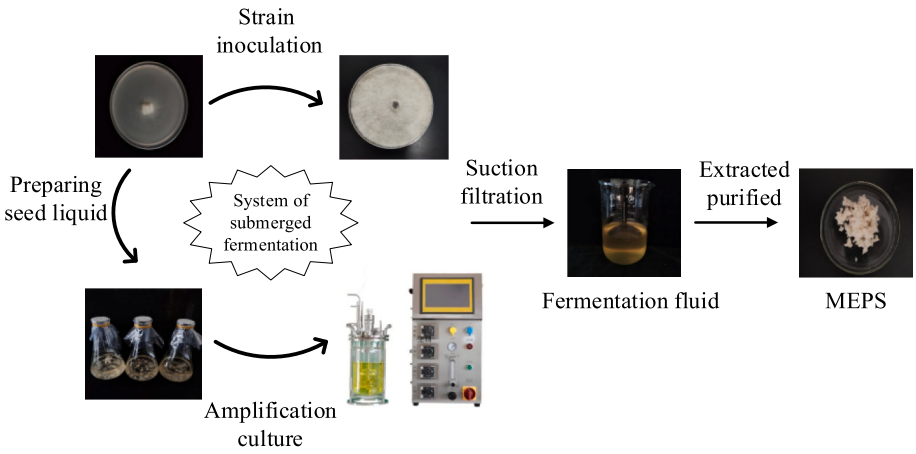

Fig. 1. Preparation of MEPS *via* submerged fermentation.

Owing to the special structure of polysaccharides, their degradation ability showed significant differences at different digestion processes in the human body. Previous studies have shown that the pH, bile salts, and digestive enzymes in the mimic digestive juice may change the physicochemical properties and active function of polysaccharides (Chen et al., 2016).

But for a few polysaccharides from *Lycium barbarum* and *Gracilaria lemaneiformis,* it has been found that their physicochemical properties did not change (Ding et al., 2019; Han et al., 2020).Previous studies in our laboratory have found that the extracellular polysaccharide from *Morchella esculenta* by submerged fermentation (MEPS) showed strong starch digestive enzyme inhibition and has a potential hypoglycemic effect (Guo et al., 2024). However, the digestion and fecal fermentation behavior of MEPS and the hypoglycemic mechanism are still unclear. Hence, this study intends to evaluate the changes in physicochemical properties and hypoglycemic activity of MEPS through the simulated digestion *in vitro*. More importantly, based on the IR-HepG2 cell model and the fecal fermentation model, its hypoglycemic mechanism was further revealed from the gene level and gut microbiota perspective using the qRT-PCR method and 16S rRNA sequencing techniques.

2. Materials and methods

2.1. Materials and reagents

The *Morchella esculenta* strain (No. CICC14033) was purchased from China Center of Industrial Culture Collection, Beijing, China. Dulbecco's modified eagle medium (DMEM) and fetal bovine serum (FBS) were acquired from Gibco, CA, USA. Pepsin, pancreatin, trypsin and L-cysteine hydrochloride were purchased from Beijing Solarbio Science & Technology Co. Ltd., Beijing, China. Acarbose, α-amylase, α-glucosidase, pig bile salt, hemin, vitamin k1, insulin and metformin were acquired from Shanghai Yuanye Bio-Technology Co. Ltd., Shanghai, China. All other chemicals and reagents used in this study were of analytical grade.

2.2. Preparation of the MEPS

The preparation of extracellular polysaccharides from *Morchella esculenta* by submerged fermentation is shown in Fig. 1. The *Morchella esculenta* strain was activated on potato dextrose agar (PDA) medium. Four pieces of mycelia cakes were inoculated in potato dextrose broth (PDB) medium (25 °C, 4 days) to prepare seed liquid. Then, the extracellular polysaccharide fermentation process was carried out in a 5 L automatic fermenter for five days. The fermentation fluid was concentrated to 1/10 of the original volume under reduced pressure (0.07–0.08 MPa), then 3× the volume of 95 % ethanol was added and the polysaccharide precipitate was isolated after overnight storage in the refrigerator at 4 °C.

Then, the polysaccharide precipitate was dissolved in distilled water, mixed with one-quarter volume of Sevag reagent (chloroform: *n*-butanol, 4:1 *v*/v) to remove protein, and this process was repeated until no white precipitate appeared. Then, the resulting liquid was dialyzed and lyophilized to obtain the crude polysaccharide.

The 10 mg/mL crude polysaccharide solution was prepared and loaded in DEAE-52 cellulose column (2.5 × 50 cm) after the impurities were removed by 0.45 μm filters (Solarbio Science & Technology Co., Ltd., Beijing, China). Distilled water and NaCl solutions (0.1–0.5 M) were used as elution solutions. 0.1 M NaCl elution fraction were collected, concentrated, and loaded on a Sephadex G-75 gel permeation column (2.5 × 50 cm), distilled water was used as elution solution. And then the polysaccharide fractions were detected, dialyzed and lyophilized. The final purified product was named MEPS.

2.3. Simulated saliva-gastrointestinal digestion

Pre-preparation of the simulated salivary (SS), simulated gastric (SG) and simulated intestinal (SI) electrolyte solutions were prepared according to the previous method with minor modifications (Ma et al., 2022).

2.3.1. Salivary digestion

α-Amylase (0.5 g) was dissolved in in 100 mL SS to prepare the salivary digestion model. Then, the MEPS solution (10 mg/mL) was mixed with the salivary model that was preincubated at 37 °C (1:2, *v*/v) in a thermostatic shaker (Shanghai Yiheng Technology Co., Ltd., Shanghai, China). Afterwards, the obtained salivary digestive mixture was incubated at 37 °C for 2 min.

2.3.2. Gastric digestion

Pepsin (0.035 g) was dissolved in 100 mL SG to prepare the gastric digestion model, then 100 mL of simulated gastric solution was mixed with an equal volume of salivary digestive mixture, and this mixture was cultured at 37 °C for 2 h.

2.3.3. Intestinal digestion

Trypsin (0.015 g) and pig bile salt (0.40 g) were dissolved in 100 mL SI to prepare the simulated intestinal fluid digestion model, then mixed with the simulated gastric digestion mixture (3:10, *v*/v). The mixture was then cultured at 37 °C for 2 h.

2.3.4. Treatment of saliva-gastrointestinal digestion products

The above digestive mixture of the salivary, gastric and intestinal stages was boiled in a 100 °C hot water for 5 min to deactivate the enzyme. The supernatant was obtained by centrifugation at room

temperature (8000 rpm, 5 min) to measure the reducing sugar concentration using the DNS method. Furthermore, the residual supernatant after dialysis and lyophilization was used for subsequent analysis of the physicochemical properties and activity. In the blank group, distilled water was used instead of polysaccharides, and the salivary, gastric and intestinal digestive products were named MEPS-S, MEPS-G and MEPS-I, respectively.

2.4. In vitro fecal fermentation of MEPS

The basal nutrient medium was prepared according to the previous method with slight modifications (Tian et al., 2023b), the MEPS-I that could not be digested was further employed for *in vitro* fecal fermentation. Eight healthy volunteers (four females and four males) aged 20–25 years who had not taken any antibiotics within the last six months provided fecal samples. Basal medium (9.0 mL) containing 100.0 mg polysaccharide was mixed with fecal slurry (1.0 mL) to initiate simulated large intestine fermentation. Under the same conditions, the medium containing fructo-oligosaccharides (FOS) was used as positive control. Samples were collected after 6 h, 12 h, 24 h and 48 h of fecal fermentation and labeled as MEPS-I-F6, MEPS-I-F12, MEPS-I-F24 and MEPS-I-F48, respectively. Then, the above samples were stored at −80 °C in a freezer for subsequent experiments and each treatment was repeated three times.

2.5. Physicochemical properties analyses

2.5.1. Analysis of the chemical components

Total carbohydrate content was assessed using the phenol-sulfuric acid method with D-glucose as the standard (Yuan et al., 2020). Protein content was determined by the Coomassie brilliant blue method with bovine serum albumin (BSA) as the standard. The uronic acid (UA) content was measured with D-galacturonic acid as standard (Blumenkrantz & Asboe-Hansen, 1973). The reducing sugar content was determined by the 3,5-dinitrosalicylic acid (DNS) method with D-glucose as standard.

2.5.2. Determination of the monosaccharide composition

The method of high-performance anion-exchange chromatography (HPAEC) was used to measure the monosaccharide composition. Polysaccharide samples were hydrolyzed with trifluoroacetic acid (2 M), after drying by nitrogen and washing 2–3 times with methanol. The residue was dissolved in deionized water (1 mL) and filtered through a 0.22 μm microporous membrane for subsequent analysis.

2.5.3. Determination of the molecular weight

The polysaccharide sample with a concentration of 1 mg/mL was prepared with a mixture of 0.02 % sodium azide (NaN3) and 0.1 m sodium nitrate (NaNO3), and filtered through a 0.45 μm pore size filter membrane. The SEC-MALLS-RI liquid phase system U3000 and Optilab T-rEX differential detector (Thermo Fisher Scientific) were used for the determination.

2.5.4. Evaluation of bioactivities

The inhibitory activity of different polysaccharide samples against α-amylase and α-glucosidase were determined according to previous reports (Cao, Huang, Zhang, Li, & Fu, 2018; Ren et al., 2017). According to the previous method, the concentration of polysaccharide sample was determined to be 8 mg/mL (Dou, Chen, & Fu, 2019).

2.6. Analysis of the hypoglycemic mechanism

2.6.1. Cell culture and cytotoxicity assay

Cells were transferred to a T25 cell culture flask containing DMEM complete medium and placed in a carbon dioxide incubator (5 % CO2, 37 °C) for culture. The viability of the HepG2 cells was detected by the CCK-8 kit (Biosharp, Beijing, China). After treatment with different concentrations of MEPS-I (2 mg/mL - 10 mg/mL) samples for 24 h and 48 h, viability was determined as a percentage of the untreated control group. The group without the HepG2 cell system served as the blank control. Under normal conditions, the medium was changed daily and when the cell density reached 80 % - 90 %, cell passage and other experiments were performed.

2.6.2. Establishment of the IR-HepG2 cell model

HepG2 cells were seeded in 96-well plates at a density of 1×10^5 cells/well, and the cells grew on the wall. When the cells grew to 80 % - 90 % confluence, the experiment was performed. DMEM with different concentrations of insulin (10–5 mol/L, 10–6 mol/L, 10–7 mol/L, 10–8 mol/L) replaced the old medium to induce culture for 12 h, 24 h, 36 h, 48 h, and 60 h, respectively. Then, the glucose content in the supernatant of the sample was determined using a glucose kit (Nanjing Jiancheng Institute of Biological Engineering, Nanjing, China). The significant difference in glucose content was considered to be a successful IR model.

2.6.3. Glucose uptake assay

After inoculation and modeling according to the methods of 2.6.1 and 2.6.2, the old medium was replaced with fresh medium containing different concentrations of MEPS-I. Then, the glucose content in the supernatant was determined after 24 h of culture. The positive control was metformin (MET) (4 mg/mL) as the carbon source, the blank group only contained medium and the negative control group was normal growth of HepG2 cells.

2.6.4. Quantitative real-time PCR (RT-PCR) analysis

QRT-PCR analyses were performed with reference to previous methods and in conjunction with the kit instructions (Sun et al., 2024). Total RNA of the treatment groups was isolated using Trizol reagent (Tiangen Biotech Co. Ltd., Beijing, China), and reverse transcription was performed using the cDNA reverse transcription kit (Tiangen Biotech Co. Ltd., Beijing, China). All primers were designed by Primer 5.0 software and synthesized by Beijing Qingke Biotechnology Co. Ltd., Beijing, China. SYBR ® GREEN Pro Taq HS qPCR Kit (Accurate Biotechnology Co. Ltd., Hunan, China) was used for the RT-PCR analysis. The primer sequences of phosphatidylinositol 3-kinase (PI3K), glucose transporter 4 (GLUT4), adenosine 5′-monophosphate (AMP)-activated protein kinase (AMPK), protein kinase B (AKT) are shown in supplementary information Table s1. Glyceraldehyde-3-phosphate dehydrogenase (GAPDH) was used as the internal standard, the relative gene expression was calculated using the 2-ΔΔCt method.

2.6.5. Analysis of pH, SCFAs during in vitro fermentation

The pH value of the fermentation samples at different fermentation times was determined by a pH meter (Inase Scientific Instrument Co., Ltd., Shanghai, China).

Single and total SCFA content at different fermentation times was determined by Shimadzu GCMS-QP2020 NX (Shimadzu, Kyoto, Japan), using 2-methylvaleric acid as the internal standard. In brief, after adding 0.2 mL H_2SO_4 (50 %, *v*/v) and 0.1 mL internal standard (0.79 mM) to 2 mL of fermentation broth, the mixture was vortexed for 5 min and then placed at 4 °C for 1 h. Then, 2 mL ethyl acetate was added. After centrifugation (8000 rpm, 10 min), the upper organic phase was taken for GC/MS analysis. An OV-1701 capillary column (30 mm × 0.25 mm × 0.50 μm) was used. The injection volume was 1 μL, and the injection port temperature was 250 °C. The heating procedure was as follows; Temperature: 40 °C for 3 min, 4 °C/min to 230 °C, hold for 2 min. Each sample was detected three times independently.

2.6.6. Analysis of gut microbiota

After 48 h fermentation, the total bacterial DNA was extracted using MagBeads FastDNA Kit for Soil kit (116564384) (MP Biomedicals, CA,

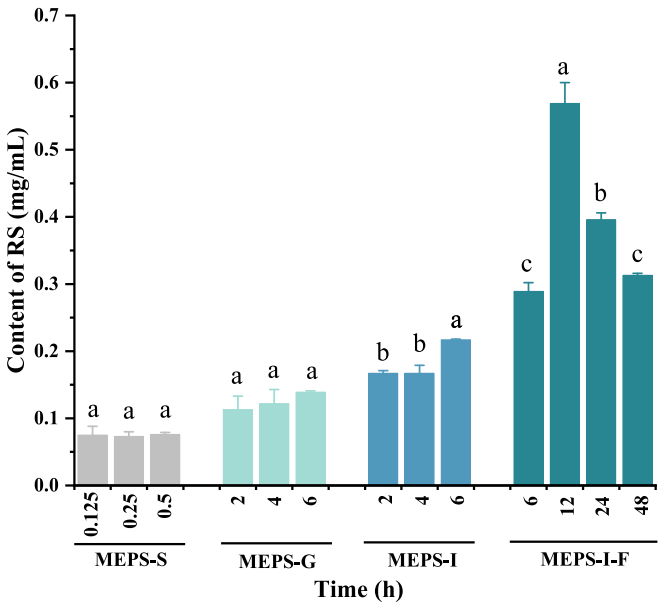

Fig. 2. Changes in RS contents of MEPS *in vitro* digestion and fermentation process.

USA), and the V3-V4 region of the bacterial 16S rDNA was sequenced and analyzed by Shanghai Pasenuo Biotechnology Co. Ltd., Shanghai, China. All results were based on sequenced reads and Amplicon Sequence Variants (ASVs).

2.7. Statistical analysis

All measurements were carried out in triplicate and the results are presented as the mean ± standard deviation (SD). ANOVA in accordance with Duncan's multiple comparisons was carried out using the IBM SPSS Statistics 27. $P < 0.05$ indicated statistical significance. Origin 2021 software (OriginLab Corporation, USA) was used for drawing. The results of the microbial diversity analysis data were plotted using tools such as QIIME2 (2019.4), R language, python language, ggplot2 packages, scikit-bio packages and Venn diagram packages.

3. Results and discussion

3.1. Variations in physicochemical characteristics and hypoglycemic activity of MEPS during in vitro digestion and fermentation

3.1.1. Changes in reducing sugar (RS) contents of MEPS

Variation in reducing sugar content during *in vitro* digestion and fermentation process can reflect the degree of damage to the glycosidic bond in polysaccharides by digestive enzymes. Fig. 2 shows the Changes in RS contents of MEPS *in vitro* digestion and fermentation process. The RS content in MEPS did not change obviously during salivary digestion, the content of RS was only about 0.07 mg/mL, which shows that MEPS is not easily degraded during saliva digestion. Whereas the content of RS significantly increased to 0.217 mg/mL ± 0.001 mg/mL within gastrointestinal digestion compared with saliva digestion, indicating that MEPS underwent slight hydrolysis during digestion due to the acidic environment. In general, some parts of the non-starch cell wall, such as polysaccharides, cannot be catalyzed by digestive enzymes, but lower pH can promote slight polysaccharide hydrolysis (Li et al., 2018). After 48 h of fecal fermentation, the RS content in MEPS was 0.313 mg/mL ± 0.003 mg/mL, which was considerably higher than that in MEPS-I (0.217 mg/mL ± 0.001 mg/mL).

Previous studies have shown that gut microbiota can encode carbohydrate-active enzymes (CAZymes) that can degrade polysaccharides, Among them , glycoside hydrolases are the largest and best studied class of CAZymes responsible for carbohydrate degradation, it can destroy glycosidic bonds in polysaccharides causing hydrolysis of polysaccharides and resulting in a significant increase in reducing sugar content (Porter & Martens, 2017; Wardman, Bains, Rahfeld, & Withers, 2022).

3.1.2. Variation in chemical composition of MEPS

Determining the chemical composition of polysaccharides in the gastrointestinal tract is of great significance for evaluating their biological activity and determining their bioavailability. The Changes in digestibility, fermentability and chemical composition of MEPS at different *in vitro* simulated digestion and fermentation stages are shown in Table 1. It can be seen that the total carbohydrate content in MEPS was 74.88 % ± 1.28 %, while the protein and uronic acids contents were 6.38 % ± 0.47 % and 2.48 % ± 0.06 %, respectively, indicating that MEPS contains a large number of polysaccharides. Due to the MEPS being degraded by bile, enzymes and pH of the gastrointestinal digestive system during the digestion process (Wang et al., 2019), accompanied by a gradual decrease in polysaccharide and uronic acids contents, its final digestibility was 22.57 %. After 48 h of *in vitro* fecal fermentation, the fermentability of MEPS gradually increased to 76.89 %, the uronic acids and total carbohydrate contents decreased by 51.21 % and 22.43 %, respectively, corresponding to the changes in reducing sugar content in Fig. 2 above. This further indicated that the indigestible MEPS can be degraded and utilized by gut microbiota.

To further analyze the digestion and fermentation characteristics of MEPS, and to evaluate its biological activity, the final saliva-gastrointestinal digestion product, MEPS-I, and fermentation product, MEPS-I-F48, selected to determine the changes in physicochemical properties, hypoglycemic activity and intestinal regulatory function.

3.1.3. Changes in monosaccharide composition, molecular weight and hypoglycemic activity of MEPS

The changes in monosaccharide composition and molecular weight

Table 1
Changes in digestibility, fermentability and chemical composition of MEPS at different *in vitro* simulated digestion and fermentation stages.

	In vitro digestion of MEPS				*In vitro* fecal fermentation of MEPS-I			
Index (%)	MEPS	MEPS-S	MEPS-G	MEPS-I	MEPS-I-F6	MEPS-I-F12	MEPS-I-F24	MEPS-I-F48
Digestibility/ fermentability	-	9.62	15.27	22.57	38.78	42.30	53.51	76.89
Total carbohydrate	74.88 ± 1.28^{a}	73.81± 2.62^{ab}	71.37± 1.66^{bc}	69.60± 2.83^{cd}	66.75± 1.25^{de}	64.02± 0.78^{e}	60.36± 2.0^{f}	58.83± 1.60^{f}
Total uronic acids	2.48± 0.06^{a}	2.27± 0.05^{b}	2.19± 0.06^{bc}	2.09± 0.08^{bc}	2.02± 0.30^{cd}	1.84± 0.07^{de}	1.76± 0.07^{e}	1.21± 0.13^{f}
Proteins	6.38± 0.47^{a}	5.41± 1.04^{a}	5.23± 2.56^{a}	6.78± 4.64^{a}	6.91± 0.17^{a}	6.32± 0.42^{a}	5.45± 0.42^{a}	6.89± 1.28^{a}

Notes: MEPS-S, MEPS-G and MEPS-I, MEPS digested by salivary digestion, saliva-gastric digestion and saliva-gastrointestinal digestion, respectively; MEPS-I-F6, MEPS-I-F12, MEPS-I-F24 and MEPS-I-F48, MEPS-I after *in vitro* fermentation for 6 h, 12 h, 24 h and 48 h, respectively.

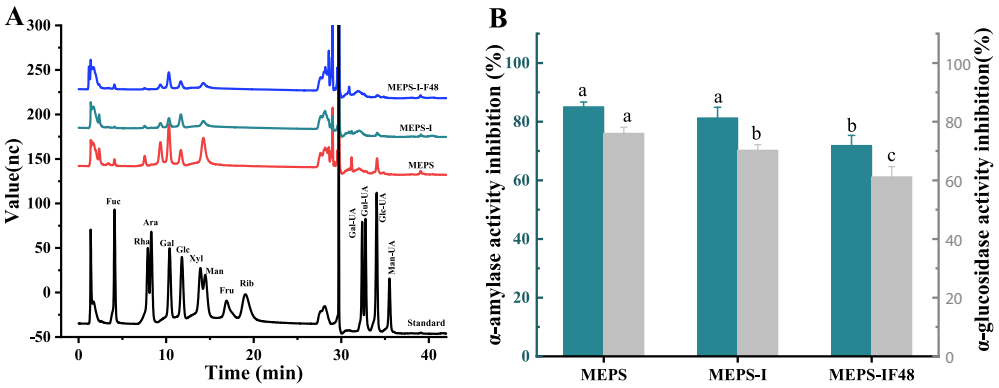

Fig. 3. Changes in the characteristics and activity of MEPS during *in vitro* digestion and fermentation. (A) HPAEC chromatograms of changes in monosaccharide composition of polysaccharide during *in vitro* digestion and fermentation; (B) Inhibitory effects on α-amylase and α-glucosidase.

Table 2
Effects of *in vitro* digestion and fermentation on molecular weight (Mw) and constituent monosaccharides of MEPS.

	MEPS	MEPS-I	MEPS-I-F48
Mw (kDa)	121.168	71.513	50.772
Constituent monosaccharide and molar ratios (%)			
Fucose (Fuc)	2.97	1.57	5.95
Galactose (Gal)	30.07	22.33	38.76
Glucose (Glc)	14.57	41.61	23.54
Mannose (Man)	44.47	27.79	27.06
Glc-Uronic Acid (Glc-UA)	7.92	6.70	4.70

of MEPS can intuitively reflect its degradation and utilization grade by enzymes and gut microbiota in the digestive system. From Fig. 3A and Table 2, the monosaccharide composition profiles of MEPS, MEPS-I and MEPS-I-F48 were similar, which were composed of Fuc, Gal, Glc, Man and Glc-UA with different molar ratios. After digestion and fermentation *in vitro,* the MEPS molecular weight decreased from 121.168 kDa to 50.772 kDa. We presumed that these results may be due to the involvement of different digestive enzymes and the pH environment during different digestion stages, as well as the involvement of gut microbes at the fecal fermentation stage, which disrupt the internal MEPS glycosidic bonds, alter its degree of branching and lead to the release of monosaccharides from some branched chains into the digestive and fermentation fluid (Geng et al., 2023). Wang et al. (2018) also found that polysaccharides from *Inonotus obliquus* underwent aggregate destruction

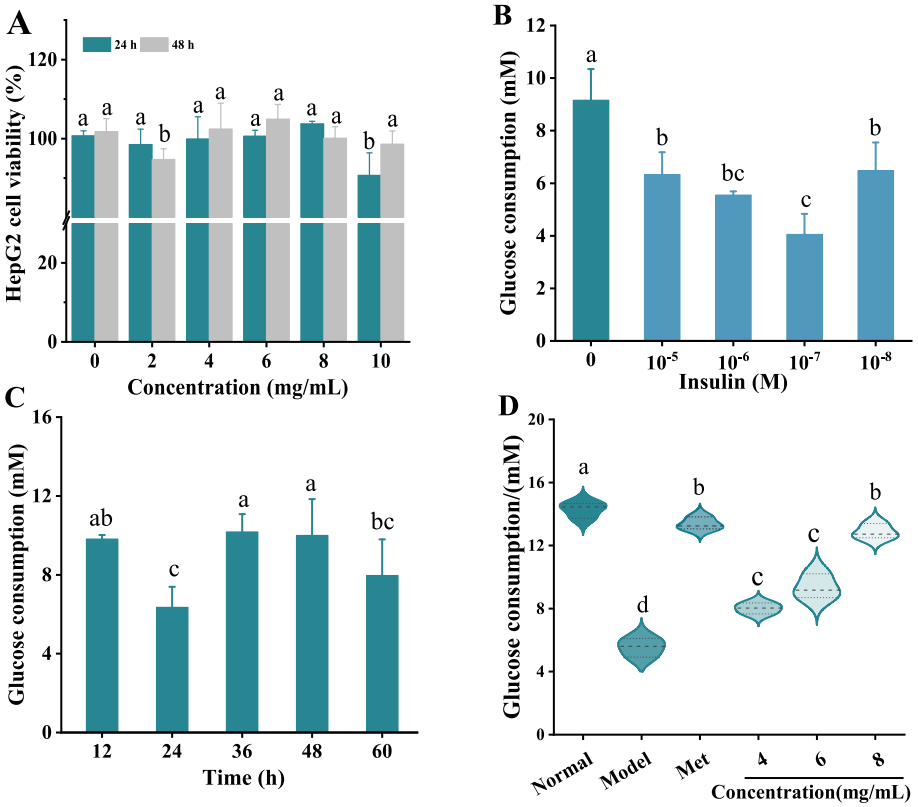

Fig. 4. The establishment of the IR HepG2 cell model and effect of MEPS-I on HepG2 cell viability and glucose consumption. (A) Effect of MEPS-I on IR-HepG2 cell viability; (B) Effect of different insulin concentrations on glucose consumption of cells under 36 h treatment conditions; (C) Effect of different incubation times on glucose consumption of HepG2 cells at 10^{-7} M insulin concentration; (D) Effect of MEPS-I on HepG2 cell glucose consumption.

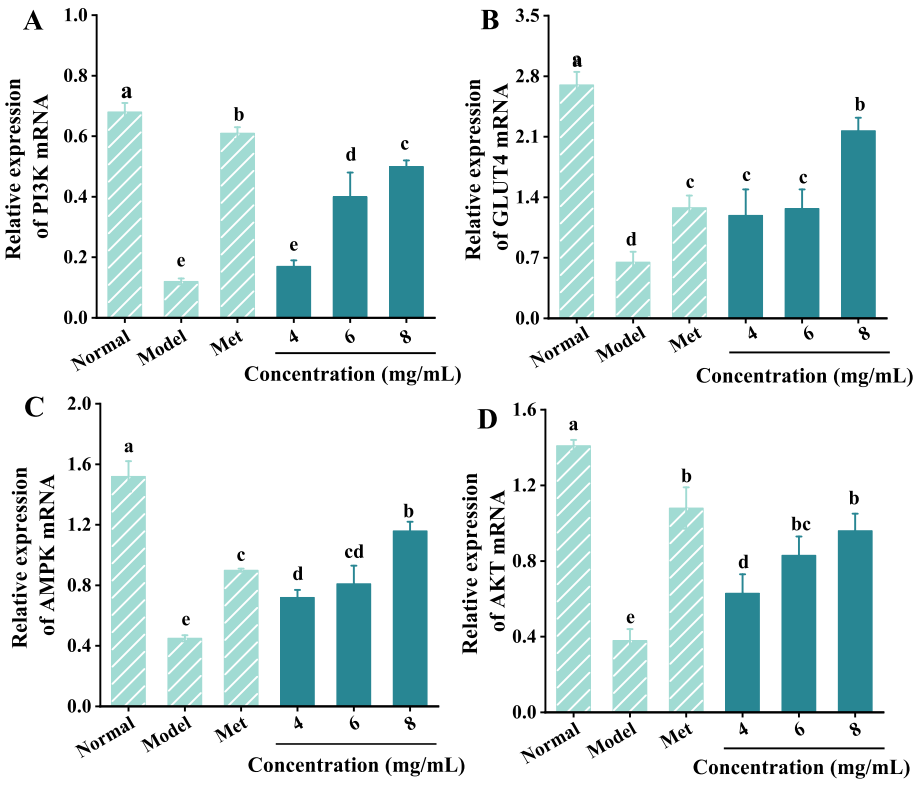

Fig. 5. Effect of MEPS-I on the activation of PI3K/AKT signaling pathways in IR-HepG2 cells. (A) PI3K mRNA; (B) GLUT4 mRNA; (C) AMPK mRNA; (D) AKT mRNA.

and glycosidic bond breakdown during simulated gastrointestinal digestion, resulting in the degradation of polysaccharides.

The physicochemical properties of polysaccharides are associated with their active functions such as anti-diabetic, anti-obesity, antioxidant, anti-inflammatory, anti-cancer and anti-aging functions (Zhang et al., 2024). To evaluate the hypoglycemic activity of polysaccharide *in vitro* simulated digestion and fermentation stages, the inhibitory effects of 8 mg/mL MEPS, MEPS-I and MEPS-I-F48 solutions on α-amylase and α-glucosidase were measured. Fig. 3B shows the changes in the inhibitory effect of MEPS on α-amylase and α-glucosidase activities during digestion and fermentation *in vitro*, the MEPS-I inhibition rate on α-amylase decreased by only 3.8 % when compared to MEPS, while the MEPS-I-F48 inhibition rate decreased by 13.19 %. The MEPS-I and MEPS-I-F48 inhibition rates on α-glucosidase were 5.76 % and 14.85 % lower than that of MEPS, respectively. This indicated that MEPS can maintain high digestive enzyme inhibitory activity during *in vitro* digestion and fermentation, especially its inhibitory effect on α-amylase, and can enter the intestine to exert its activity. However, it has been reported that the α-glucosidase and α-amylase inhibitory activities of Tea polysaccharides (TPS) and *Opilia amentacea* fruit polysaccharides (OAFP) were significantly enhanced after gastrointestinal digestion (Kasipandi et al., 2019; Li, Wang, Yuan, Pan, & Chen, 2018). This difference may be related to the degree of glycosidic bond breakdown and the different types of monosaccharides produced after partial hydrolysis of polysaccharides.

3.2. Analysis of the hypoglycemic mechanism of MEPS-I

3.2.1. Effect of MEPS-I on HepG2 cell viability and glucose consumption

Insulin resistance can damage the liver, muscle and other peripheral tissues involved in blood glucose metabolism, causing blood glucose metabolism disorders in the body and increasing blood glucose concentration (Nolan, Ruderman, Kahn, Pedersen, & Prentki, 2015). HepG2 cells have the morphology and metabolic function of normal liver cells and maintain most liver functions, it is an ideal cell model for studying and developing potential hypoglycemic drugs and exploring hypoglycemic mechanisms *in vitro*. In this study, the IR-HepG2 cell model was established to evaluate the hypoglycemic activity and mechanism of MEPS-I at the molecular level. Fig. 4A shows the effect of MEPS-I on IR-HepG2 cell viability. When the concentration of MEPS-I was 4 mg/mL, 6 mg/mL and 8 mg/mL, there was no significant difference in the proliferation rate of the HepG2 cells when compared with the control group. Therefore, 4 mg/mL, 6 mg/mL and 8 mg/mL doses were used for subsequent experiments, which were named MEPS-I-LD, MEPS-I-MD and MEPS-I-HD, respectively.

The results of the IR-HepG2 cell model establishment are shown in Fig. 4B and C. The sensitivity of HepG2 to insulin was weakened and glucose could not be effectively absorbed and utilized, resulting in insulin resistance when HepG2 cell is cultured at 10–7 M insulin concentration for 24 h. Therefore, the subsequent experiments were conducted to construct an IR HepG2 cell model by incubating HepG2 cells with insulin at a concentration of 10^{-7} mol/L for 24 h.

The MEPS-I effect on glucose uptake in IR HepG2 cells is shown in Fig. 4D. The glucose uptake of IR-HepG2 cells was 5.54 mM in the model group, which was much lower than that of normal HepG2 cells (14.28 mM), indicating that the model was successfully established. After being treated with MEPS-I-LD, MEPS-I-MD and MEPS-I-HD for 24 h, compared to the model group, glucose uptake in the IR-HepG2 cells was significantly increased in a dose-dependent manner by 44.57 %, 68.74 %, and 132.13 %, respectively, but lower than that of the positive control (141.34 %). The results indicated that MEPS-I can improve insulin resistance, regulate glucose metabolism, and increase glucose utilization in HepG2 cells. The potential mechanism may be related to the activation of insulin signaling pathway and the increased expression of glucose transporters. For example, Xie et al. (2022) found that Polysaccharides from *Enteromorpha prolifera* improves insulin sensitivity in diet-induced obese mice associated with activation of PGC-1α-FNDC5/irisin pathway. Ganoderma lucidum polysaccharides significantly upregulated the mRNA and protein levels of GLUT4 and GS, thereby promoting glucose uptake and glycogen synthesis (Liu, Li, Zhang, Sun, & Zhang, 2019).

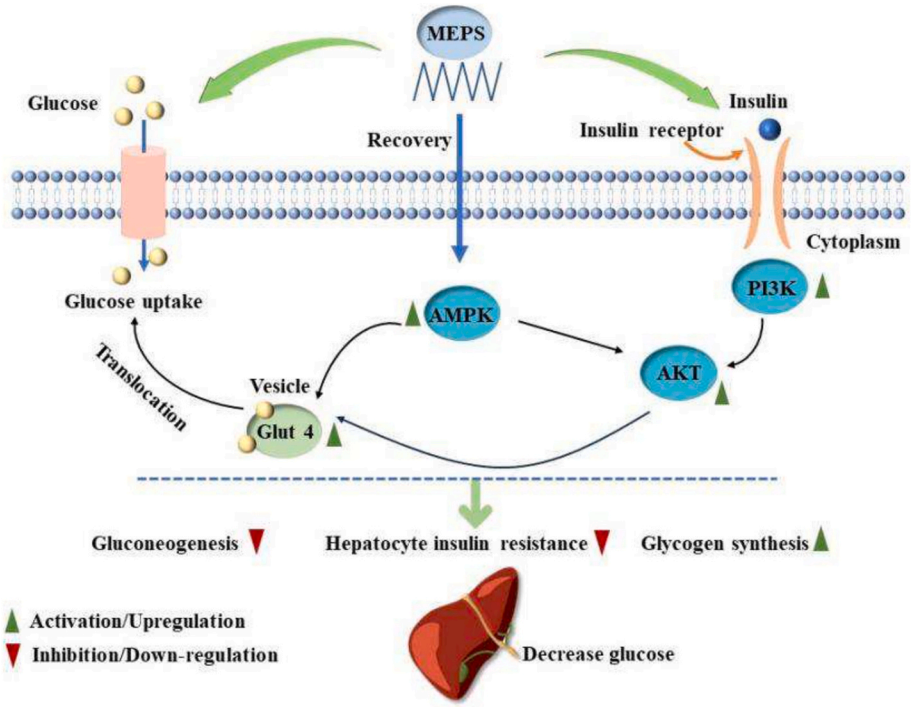

Fig. 6. The schematic of MEPS ameliorated insulin resistance by regulating the PI3K/AKT/ GLUT4/AMPK insulin signaling pathway.

3.2.2. Effect of MEPS-I on the PI3K/AKT signaling pathways of glycolipid metabolism pathway

Enhancing the biological effects of insulin is considered to be an effective way to treat IR, mainly through the transduction of insulin receptor activation, insulin receptor substrate phosphorylation, and other signaling pathways (Su, Tang, Luo, Xu, & Ouyang, 2023). At present, the research on the mechanism of IR is mostly focused on the level of insulin receptor, especially the PI3K/AKT signaling pathway, which are the main pathways to regulate glycolipid metabolism in adipose tissue and plays a critical role in insulin signal perception and transduction (Feng, Liu, Xing, Zhong, & Zhou, 2021; Liu et al., 2023).

PI3K is a lipid kinase that mediates insulin metabolism. AKT is generally considered one of the main factors that initiate cellular signaling in the PI3K signaling pathway. GLUT4 is one of the important glucose transporters downstream of the PI3K/AKT signaling pathway. It can not only transport glucose to fat and muscle cells, but also uptake glucose to insulin reaction sites, thereby promoting cells uptake and utilization of glucose (Liu et al., 2020; Xiao et al., 2018). The activity, translocation and expression of GLUT4 are the key causes of insulin resistance in adipose tissue and IR caused by insulin signal blocking. In addition, AMPK, another important energy-sensing and metabolic regulator, is a serine/threonine kinase that initiates the PI3K/AKT signaling pathway and enhances insulin sensitivity (Zhou et al., 2021). The AMPK signaling pathway has been considered as a potential therapeutic target for the treatment of various diseases. Li et al. (2020) found that sesquiterpene glycosides (SGs) enhanced glucose metabolism and uptake in IR-HepG2 cells by stimulating AMPK signaling. In addition, AMPK can also affect renal inflammation, reduce renal cell apoptosis and increase GLUT4 expression by regulating the PI3K/AKT pathway, leading to a significant increase in glucose uptake (Entezari et al., 2022). Fig. 5 shows the changes in mRNA expression of PI3K, GLUT4, AMPK and AKT genes of IR-HepG2 cells after MEPS-I intervention. The mRNA expression of the four genes in the model group were significantly decreased compared to those of the blank group ($p < 0.05$), showing that the model was successful. However, the expression levels of PI3K, GLUT4, AMPK and AKT in IR-HepG2 cells were significantly increased compared to the model group after MEPS-I induction. In summary, the

Table 3
Changes in pH and the contents of SCFAs at different time points of fermentation.

Treatment	Time (h)	pH	Short-chain fatty acids (mmol/L)			
			Acetic acid	Propionic acid	Butyric acid	Total
BLANK	0	7.12 ± 0.3$^{a, A}$	2.64 ± 1.75$^{d, A}$	0.09 ± 0.05$^{c, A}$	0.12 ± 0.11$^{b, A}$	2.86 ± 1.60$^{d, A}$
	6	7.02 ± 0.11$^{ab, A}$	4.34 ± 3.12$^{cd, B}$	0.46 ± 0.06$^{b, A}$	0.18 ± 0.01$^{b, A}$	4.98 ± 3.17$^{cd, B}$
	12	6.86 ± 0.14$^{bc, A}$	9.93 ± 1.48$^{bc, B}$	0.94 ± 0.24$^{a, A}$	0.18 ± 0.03$^{b, B}$	11.05 ± 1.71$^{bc, B}$
	24	6.79 ± 0.13$^{bc, A}$	14.19 ± 5.88$^{b, B}$	0.97 ± 0.16$^{a, A}$	0.22 ± 15.39$^{b, A}$	15.39 ± 6.00$^{b, B}$
	48	6.70 ± 0.19$^{c, A}$	21.09 ± 4.50$^{a, C}$	1.14 ± 0.14$^{a, B}$	0.52 ± 0.07$^{a, A}$	22.75 ± 4.68$^{a, C}$
FOS	0	7.02 ± 0.22$^{a, A}$	5.09 ± 2.21$^{d, A}$	0.24 ± 0.21$^{c, A}$	0.11 ± 0.10$^{b, A}$	5.44 ± 2.33$^{d, A}$
	6	5.41 ± 0.2$^{b, C}$	12.34 ± 3.84$^{cd, A}$	0.38 ± 0.03$^{c, A}$	0.20 ± 0.06$^{b, A}$	12.91 ± 3.94$^{d, A}$
	12	4.52 ± 0.13$^{c, C}$	20.13 ± 4.22$^{c, A}$	1.65 ± 0.60$^{b, A}$	0.28 ± 0.02$^{b, B}$	22.06 ± 4.77$^{c, A}$
	24	3.93 ± 0.02$^{d, C}$	28.60 ± 6.01$^{b, A}$	1.78 ± 0.73$^{b, A}$	2.68 ± 0.81$^{ab, A}$	33.07 ± 7.21$^{b, A}$
	48	3.78 ± 0.13$^{d, B}$	45.03 ± 6.46$^{a, A}$	6.30 ± 1.35$^{a, A}$	4.84 ± 3.15$^{a, A}$	56.17 ± 4.76$^{a, A}$
MEPS-I	0	6.95 ± 0.19$^{a, A}$	2.51 ± 1.21$^{e, A}$	0.09 ± 0.01$^{b, A}$	0.15 ± 0.01$^{b, A}$	2.75 ± 1.23$^{e, A}$
	6	5.76 ± 0.14$^{b, B}$	10.29 ± 2.33$^{d, AB}$	0.41 ± 0.40$^{b, A}$	0.80 ± 0.68$^{ab, A}$	11.50 ± 1.88$^{d, A}$
	12	4.87 ± 0.11$^{c, B}$	16.05 ± 4.32$^{c, AB}$	0.97 ± 0.18$^{b, A}$	1.64 ± 0.35$^{ab, A}$	18.66 ± 4.82$^{c, AB}$
	24	4.11 ± 0.06$^{d, B}$	25.88 ± 1.81$^{b, A}$	1.00 ± 0.22$^{b, A}$	2.84 ± 3.22$^{ab, A}$	29.72 ± 5.08$^{b, A}$
	48	3.82 ± 0.11$^{e, B}$	32.16 ± 1.95$^{a, B}$	6.05 ± 6.20$^{a, A}$	2.89 ±3.29$^{a, A}$	45.56 ± 5.79$^{a, B}$

Notes: Different capital letters (A-C) indicate significant differences among different groups ($p < 0.05$) at the same fermentation time point, while different lowercase letters (a-e) represent significant differences among different fermentation times ($p < 0.05$) in the same group.

Table 4
Changes in Alpha diversity of samples between different groups.

Groups	Index				
	Chao1	Observed species	Shannon	Simpson	Coverage
BLANK	427.13 ± 30.94[a]	399.60 ± 28.98[a]	3.85 ± 0.81[a]	0.81 ± 0.04[a]	0.9989 ± 0.0001[b]
MEPS-I	278.06 ± 14.55[b]	267.93 ± 9.59[b]	3.63 ± 0.12[a]	0.84 ± 0.02[a]	0.9995 ± 0.0002[a]
FOS	246.00 ± 35.61[b]	233.73 ± 38.41[b]	3.50 ± 0.02[a]	0.83 ± 0.00[a]	0.9995 ± 0.0001[a]

Notes: Different lowercase letters (a, b and c) show significant difference among different treatment groups ($p < 0.05$) in each column by a Tukey test.

IR-HepG2 cell experiments *in vitro* showed that the extracellular polysaccharide of *Morchella esculenta* can alleviate insulin resistance and increase glucose consumption of IR cells by activating the PI3K/AKT signaling pathway and up-regulating AMPK/GLUT4 mRNA expression (Fig. 6).

3.3. *In vitro simulated fecal fermentation of MEPS-I*

3.3.1. *Effects of MEPS-I on pH and SCFAs*

The pH values of the MEPS-I and FOS groups decreased steadily during the whole fecal fermentation process and it reduced from 6.95 to 3.82 and from 7.02 to 3.78 after 48 h, respectively (Table 3). Additionally, the pH value in the MEPS-I group decreased rapidly with fermentation progression, and lower than that in the blank group at the same fermentation time. The differences in the types and quantities of gut microbes in the fermentation systems of BLANK and MEPS-I may be the main cause of the pH differences. It is well known that mildly acidic conditions allow butyrate-producing bacteria to compete against gram-negative carbohydrate-utilizing bacteria, such as *Bacteroides spp.*, which can maintain the homeostasis of the intestinal microorganisms (Colucci et al., 2024). In addition, the proliferation of harmful bacteria such as *E. coli* is inhibited in weak acidic environment (Tian et al., 2023a). Furthermore, after 12 h of fermentation, the MEPS-I group and FOS group pH values were < 5, that resulted in significant changes in the colony composition and metabolism of the intestinal microorganisms (Cao et al., 2023).

Studies have found that SCFAs are closely related to glucose homeostasis which can improve insulin sensitivity, maintain liver glucose and energy homeostasis (Gao et al., 2024). Acetic acid, the most common SCFA in peripheral circulation, can improve insulin resistance and glucose tolerance in high-fat-fed mice (Saad, Santos, & Prada, 2016). Propionic acid is mainly produced by fermentation of mannose and glucose, which can inhibit cholesterol synthesis, prevent diet-induced obesity and improve insulin sensitivity (Fu et al., 2019). Also, butyric acid is the main energy source of colonic epithelial cells, supplementation with it mainly decreases ectopic lipid deposition and inflammation, reverses obesity and insulin resistance (McNabney & Henagan, 2017). Therefore, this study further evaluated the potential effects of MEPS-I on the intestinal microenvironment by measuring the changes in the acetic acid, propionic acid and butyric acid contents during fermentation. As shown in Table 3, with the prolongation of fermentation time, the single and total SCFAs contents in each treatment group increased gradually. After 48 h fermentation, the acetic acid, propionic acid, and butyric acid contents in the MEPS-I group increased to 32.16 mmol/L ± 1.95 mmol/L, 6.05 mmol/L ± 6.20 mmol/L and 2.89 mmol/L ± 3.29 mmol/L, which were 1.52×, 5.31× and 5.56× higher than those in the blank group, respectively, and the total SCFAs concentration (45.56 mmol/L ± 5.79 mmol/L) was twice as high than that of the blank group (22.75 mmol/L ± 4.68 mmol/L). The results of SCFAs also showed that acetate production accounted for the highest proportion of total SCFAs, it can be speculated that acetate-producing bacteria should be far more abundant than propionate, butyrate-producing bacteria. In addition, the total SCFAs in MEPS-I group was significantly higher than that in the *Ophicordyceps sinensis*, *Cordyceps militaris* and *Volvariella volvacea* polysaccharide sample at the same fermentation time (Hu et al., 2023; Ji et al., 2020). In general, MEPS-I can be degraded and utilized by intestinal microorganisms to produce more SCFAs, which has a good promoting effect on the proliferation of colonic probiotics.

3.3.2. *Effects of MEPS-I on the modulation of gut microbiota*

Gut microbial imbalance is also associated with the occurrence and progression of type II diabetes (Ma et al., 2019). The high-throughput sequencing of bacterial 16S rRNA was used to explore the effects of MEPS on human fecal microbiota after 48 h fermentation. The alpha diversity index (Chao 1, Observed species, Shannon, and Simpson) results are shown in Table 4. These indices are often used to assess the

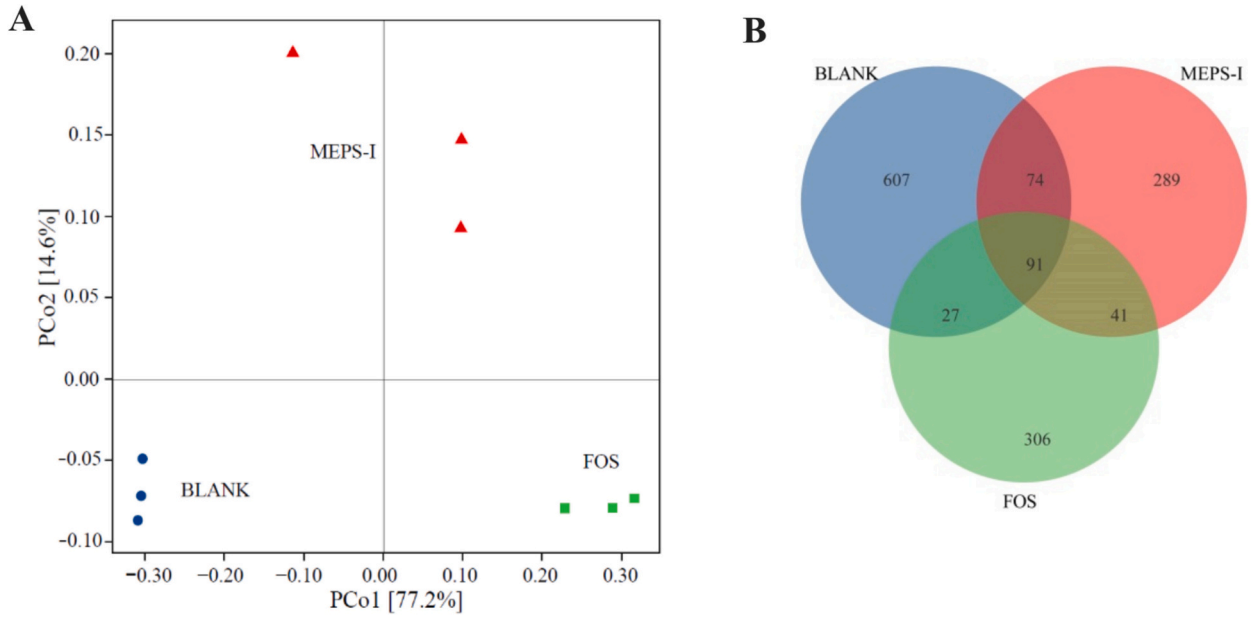

Fig. 7. Compositions of gut microbiota using β diversity analysis and Venn diagram analysis among each group. (A) Principal co-ordinates analysis (PCoA); (B)Venn diagram analysis of gut microbiota at the ASV level.

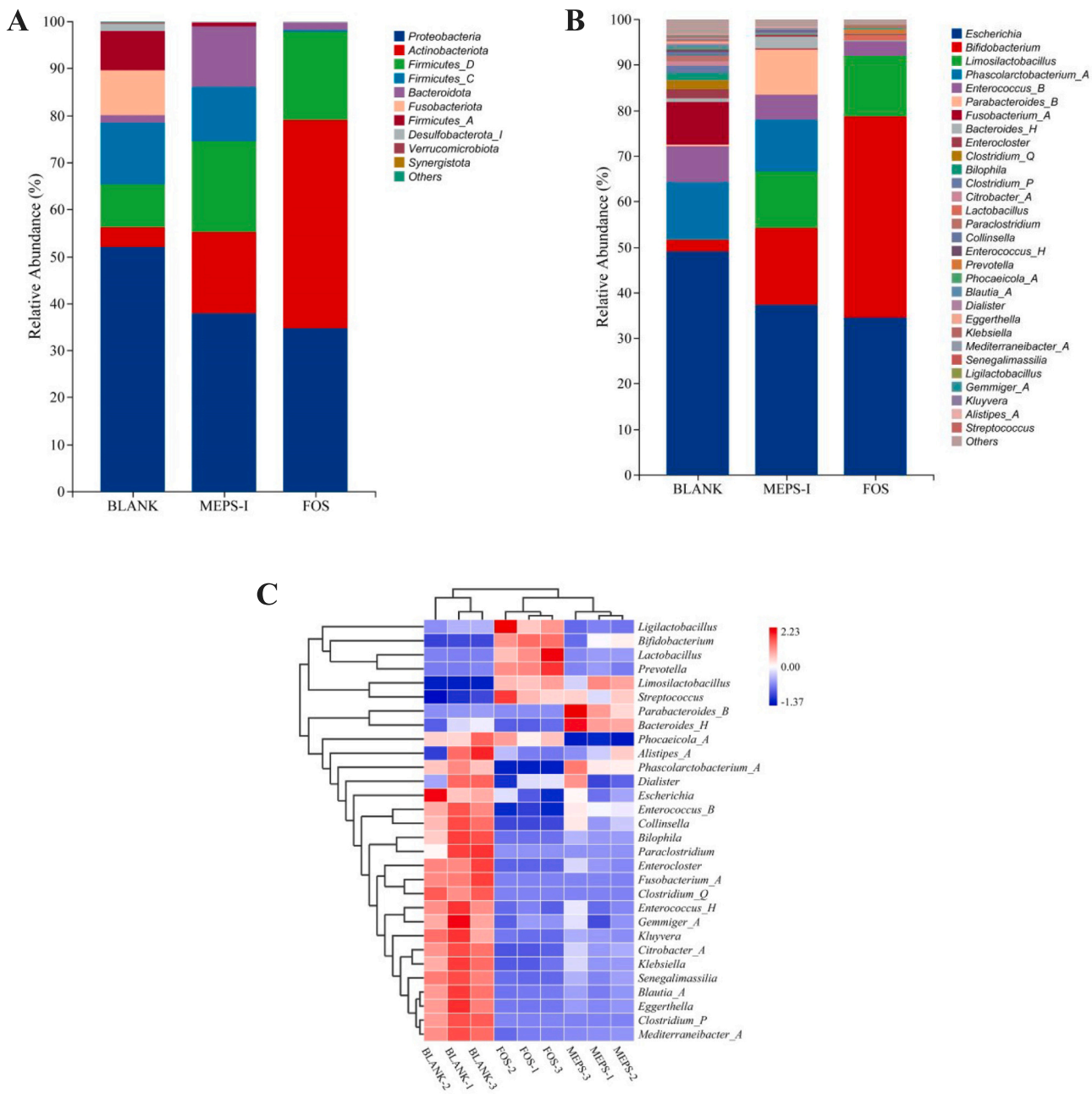

Fig. 8. Composition of gut microbiota in different treatments. (A) Bacterial taxonomic profiling at the phylum level; (B) Bacterial taxonomic profiling at the genus level; (C) The heat map analysis at genus level.

species abundance and diversity of the gut microbiota. The results showed that the Chao1 and Observed species indices of MEPS-I and FOS fermentation groups were significantly lower than those of the blank group ($p < 0.05$). Moreover, there was no significant difference in Shannon and Simpson indices, indicating that MEPS-I could reduce the richness of the microorganisms. This is consistent with the impact of polysaccharide from *Ficus carica* Linn on gut community richness (Han et al., 2022; Xu et al., 2024), which may be related to the competition of dominant flora.

Fig. 7 evaluates the microbial composition differences between different groups through β-diversity analysis and Venn diagram analysis. As shown in Fig. 7A, it shows that there is a clear clustering between gut microbiota composition obtained from the different groups and the specimens within each group clustered together. PCo1 and PCo2 contributed 77.2 % and 14.6 % of the variation, respectively. Those data demonstrated that there were significant differences in gut microbiota composition between the three groups. Thus, MEPS-I, as a special carbon source, played a vital role in regulating the growth and metabolism of gut microbiota. Besides, the Venn diagram can directly show the relationship and difference between microbial communities in different samples by comparing the similarity and uniqueness of ASV. According to the Venn diagram (Fig. 7B), there were 91 shared ASVs in the three groups, and the unique ASV counts were 607, 289 and 306 in the Blank, MEPS-I and FOS groups, respectively.

Subsequently, Fig. 8A shows the variations in gut microbiota at the phylum level. Notably, the four prevailing bacteria in the BLANK group are *Proteobacteria* (52.19 %), *Firmicutes* (31.50 %), *Fusobacteria* (9.54 %) and *Actinobacteria* (4.15 %). In comparison with the BLANK sample, the

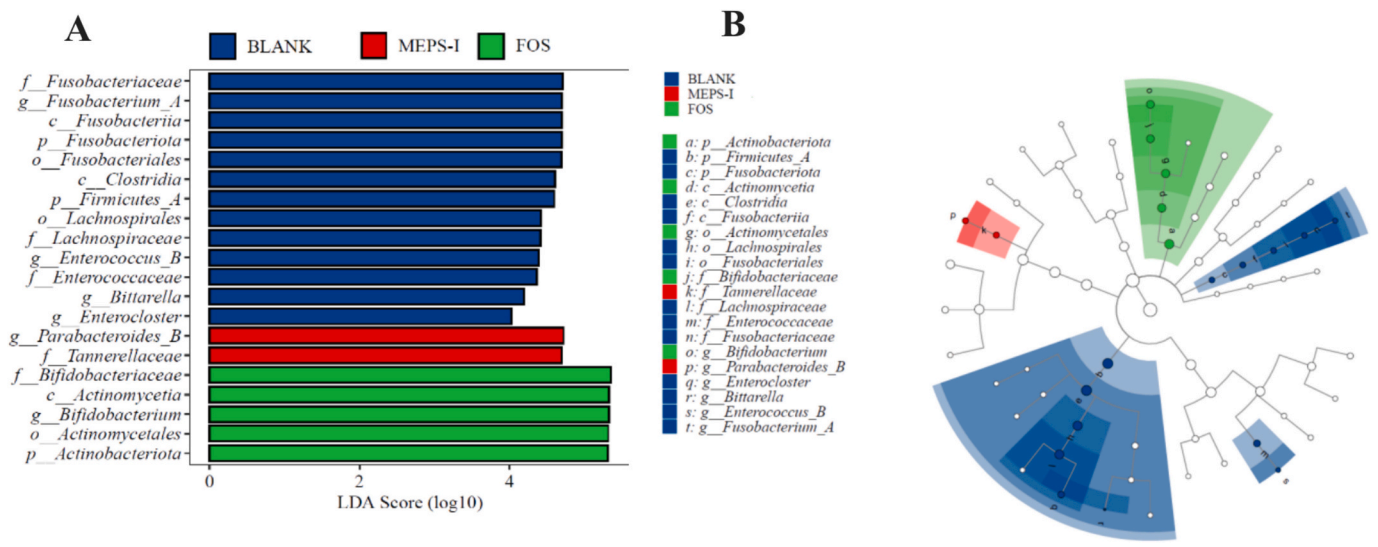

Fig. 9. Effects of MEPS-I on gut microbiota after 48 h fermentation. (A)Linear discriminant analysis (LDA) score for taxa difference; (B) Linear discriminant analysis effect size (LEfSe) evolutionary branch graph between the BLANK, MEPS-I and FOS groups.

abundance of *Bacteroidetes* in the MEPS-I group was 8 times higher than that in the blank group. *Bacteroidetes* can encode polysaccharide lyases and glycosidases genes, which can degrade polysaccharides and promote the metabolism of polysaccharides by other intestinal microorganisms to produce metabolites such as short-chain fatty acids and amino acids. Additionally, previous studies have demonstrated that the abundance of *Bacteroides* is reduced in diabetic patients (Cheng, Hu, Geng, & Nie, 2022; Niu et al., 2024). *Proteobacteria* can cause a gut microbiota imbalance and the increase in its abundance is related to the occurrence of colitis (Ren et al., 2021). The proportion of *Firmicutes* and *Bacteroides* (F/B) in the human gut was inversely associated with the risk of insulin resistance and weight gain. The result was found that the profusion of *Firmicutes* and *Proteobacteria* decreased significantly with MEPS-I fermentation and the ratio of *Firmicutes/Bacteroidetes* decreased from 18.89 (BLANK group) to 2.44 (MEPS-I group). Meanwhile, *Fusobacteria* and *Desulfobacterota* were detected in the blank group, but not in the MEPS-I and FOS group. *Fusobacterium*, a pathogen increased due to nutritional deficiencies and was reported to be associated with the development of colorectal cancer (CRC), gastric cancer and other cancers (Park, Han, Oh, Lee, & Eun, 2016). The increase of *Desulfobacterota* abundance may affect the development of some chronic complications in the late stage of diabetes (Liu et al., 2022).

The microbial community structure was also evaluated at the genus level, and the results are shown in Fig. 8B. The dominant bacteria in the BLANK group at the genus level included *Escherichia* (49.18 %), *Phascolarctobacterium*_A (12.67 %), *Fusobacterium*_A (9.51 %) and *Enterococcus*_B (7.87 %). Some clinical studies have shown that the blooms of *E. coli* and other *Enterobacteriaceae* can promote the occurrence of intestinal inflammation, and *Enterococcus* is also associated with lipid metabolism, leading to lipid metabolism disorders by disrupting intestinal permeability (Faqerah, Walker, & Gerasimidis, 2023; Liu et al., 2018). Compared with the BLANK, the relative abundances of *Escherichia*, *Fusobacterium*_A and *Enterococcus*_B in MEPS-I and FOS sample groups were significantly decreased. *Phascolarctoobacter* _ A is a potentially beneficial bacterium that inhibits obesity and is positively correlated with acetic acid content (Sun et al., 2021), and the results showed that there was no significant difference in the abundance of *Phascolarctoobacter* _ A between the MEPS-I and the BLANK groups, indicating that MEPS-I did not inhibit them.

Moreover, MEPS-I and FOS induction can significantly increase the abundance of *Limosilactobacillus* and *Bifidobacterium*. *Limosilactobacillus* can enhance intestinal barrier function, improve insulin sensitivity and glucose homeostasis by producing antibacterial substances such as organic acids and reuterin, or other various beneficial metabolites (Di Porzio et al., 2023; Wu et al., 2022). *Bifidobacterium* can hydrolyze carbohydrates and produce SCFAs, which reduce blood glucose levels in diabetic rats by improving insulin sensitivity and increasing glucose uptake (Zhang et al., 2020).

The heatmap analysis in Fig. 8C intuitively demonstrated the difference and similarity of the microbial communities between the different groups at the genus level. It showed that the microbial communities between the treatment groups were statistically separated. In addition, the predominant gut microbiota was not consistent, and the same group of samples were clustered together. The representative beneficial bacteria genera were *Limosilactobacillus*, *Bacteroides*_H and *Phascolarctobacterium*_A in the MEPS-I group. It concluded that MEPS-I significantly changed the microbial composition when compared with the BLANK group.

LEfSe was used to better display the microbiota with significant differences in abundance in each group (Fig. 9). 20 genera were above 4.0 based on linear discriminant analysis. Among them, there were 13, 2 and 5 types of ascendent genera in the BLANK, MEPS-I and FOS groups, respectively, indicating significant discrepancies in dominant bacteria among the groups. *Tannerellaceae* and *Parabacteroides*_ B were dominant genera in the MEPS-I group, which had anti-inflammatory and epithelial barrier enhancement functions. In addition, *Tannerellaceae* was positively correlated with *n*-butyric acid (Belles et al., 2022; Wang, Zhang, Li, Xu, & Chen, 2022). The proliferation of *Tannerellaceae* and *Parabacteroides*_ B induced by MEPS-I may produce more beneficial metabolites, which helps to maintain the homeostasis of intestinal function. This result was consistent with the results of *Portulaca oleracea* polysaccharides (Fu et al., 2022).

Overall, these results suggest that MEPS-I intervention can reduce harmful bacteria and promote the growth of beneficial bacteria, which play a critical role in alleviating glucose metabolism disorders caused by insulin resistance and can prevent the occurrence of diabetes by improving the composition of gut microbiota.

4. Conclusions

Herein, the digestion behavior and hypoglycemic activity of extracellular polysaccharide from *M. esculenta* were examined through the *in vitro* simulation and fermentation experiments. The results showed that MEPS were gradually hydrolyzed and promoted the production of

SCFAs, especially acetic acid, propionic acid and butyric acid after 48 h of fecal fermentation by human fecal microbiota. Meanwhile, the MEPS-I, the final product of saliva-gastrointestinal digestion still retained higher hypoglycemic activity, it alleviated IR and increased glucose consumption of IR cells by activating the PI3K/AKT signaling pathway, a key signaling pathway regulating glucose and lipid metabolism in adipose tissue. Furthermore, the MEPS-I dramatically reduced the *Firmicutes/Bacteroidetes* ratio, promoted the relative abundance of intestinal beneficial bacteria that enhanced insulin sensitivity and increased glucose uptake. It also inhibited the growth of harmful bacteria that cause lipid metabolism disorders. The result of this study indicated that MEPS is a potential functional factor to improve insulin resistance in diabetes by activating the PI3K/AKT signaling pathway and modulating the composition of the gut microbiota, which can provide a theoretical basis for the further development of morel as a health functional food.

Ethical statement

Fresh fecal samples were collected from healthy volunteers for *in vitro* testing, all participants provided informed consent before participating in the study. The anonymity and confidentiality of the participants were guaranteed, and participation was completely voluntary. Ethical permission about our study is not a requirement of my institution.

CRediT authorship contribution statement

Weihong Guo: Writing – original draft, Validation, Project administration, Methodology, Data curation. **Xuerui Wang:** Supervision, Data curation. **Biao Wang:** Software, Formal analysis. **Yajie Zhang:** Investigation. **Fengyun Zhao:** Visualization. **Yuling Qu:** Methodology. **Liang Yao:** Funding acquisition. **Jianmin Yun:** Writing – review & editing, Resources, Funding acquisition, Conceptualization.

Declaration of competing interest

There is no conflict of interests to declare.

Data availability

Data will be made available on request.

Acknowledgements

This work was supported by the Gansu Province subsidy fund project for enhancing Science and technology implemented by Ning County (NXKJ2023-02) and the financial support from Gansu Provincial Science and Technology Major Projects (21ZD4NA016).

Appendix A. Supplementary data

Supplementary data to this article can be found online at https://doi.org/10.1016/j.fochx.2024.101870.

References

Belles, A., Aguirre-Ramirez, D., Abad, I., Parras-Molto, M., Sanchez, L., & Grasa, L. (2022). Lactoferrin modulates gut microbiota and toll-like receptors (TLRs) in mice with dysbiosis induced by antibiotics. *Food & Function, 13*(10), 5854–5869. https://doi.org/10.1039/d2fo00287f

Blumenkrantz, N., & Asboe-Hansen, G. (1973). New method for quantitative determination of uronic acids. *Analytical Biochemistry, 54*(2), 484–489. https://doi.org/10.1016/0003-2697(73)90377-1

Cai, W.-D., Ding, Z.-C., Wang, Y.-Y., Yang, Y., Zhang, H.-N., & Yan, J.-K. (2020). Hypoglycemic benefit and potential mechanism of a polysaccharide from *Hericium erinaceus* in streptozotoxin-induced diabetic rats. *Process Biochemistry, 88*, 180–188. https://doi.org/10.1016/j.procbio.2019.09.035

Cao, C., Huang, Q., Zhang, B., Li, C., & Fu, X. (2018). Physicochemical characterization and *in vitro* hypoglycemic activities of polysaccharides from *Sargassum pallidum* by microwave-assisted aqueous two-phase extraction. *International Journal of Biological Macromolecules, 109*, 357–368. https://doi.org/10.1016/j.ijbiomac.2017.12.096

Cao, Z., Ding, Y., Liu, Z., Liu, M., Wu, H., Zhao, J., Dong, X., & Shang, H. (2023). Extraction condition optimization and prebiotic potential of dandelion (*Taraxacum mongolicum* hand.-Mazz.) polysaccharides. *Industrial Crops and Products, 194*, Article 116381. https://doi.org/10.1016/j.indcrop.2023.116318

Chen, C., Zhang, B., Fu, X., You, L.-J., Abbasi, A. M., & Liu, R. H. (2016). The digestibility of mulberry fruit polysaccharides and its impact on lipolysis under simulated saliva, gastric and intestinal conditions. *Food Hydrocolloids, 58*, 171–178. https://doi.org/10.1016/j.foodhyd.2016.02.033

Cheng, J., Hu, J., Geng, F., & Nie, S. (2022). *Bacteroides* utilization for dietary polysaccharides and their beneficial effects on gut health. *Food Science and Human Wellness, 11*(5), 1101–1110. https://doi.org/10.1016/j.fshw.2022.04.002

Colucci, C. R., Nigro, F., Passannanti, F., Lentini, G., Gallo, M., Nigro, R., & Budelli, A. L. (2024). Gut health benefits and associated systemic effects provided by functional components from the fermentation of natural matrices. *Comprehensive Reviews in Food Science and Food Safety, 23*(3), Article e13356. https://doi.org/10.1111/1541-4337.13356

Di Porzio, A., Barrella, V., Gatto, C., Cigliano, L., Spagnuolo, M. S., Crescenzo, R., … Mazzoli, A. (2023). Protective effect of probiotic *Limosilactobacillus reuteri* DSM17938 against western diet-induced obesity and associated metabolic alterations. *Journal of Functional Foods, 109*, Article 105805. https://doi.org/10.1016/j.jff.2023.105805

Ding, Y., Yan, Y., Peng, Y., Chen, D., Mi, J., Lu, L., Luo, Q., Li, X., Zeng, X., & Cao, Y. (2019). *In vitro* digestion under simulated saliva, gastric and small intestinal conditions and fermentation by human gut microbiota of polysaccharides from the fruits of *Lycium barbarum*. *International Journal of Biological Macromolecules, 125*, 751–760. https://doi.org/10.1016/j.ijbiomac.2018.12.081

Dou, Z., Chen, C., & Fu, X. (2019). The effect of ultrasound irradiation on the physicochemical properties and α-glucosidase inhibitory effect of blackberry fruit polysaccharide. *Food Hydrocolloids, 96*, 568–576. https://doi.org/10.1016/j.foodhyd.2019.06.002

Entezari, M., Hashemi, D., Taheriazam, A., Zabolian, A., Mohammadi, S., Fakhri, F., … Samarghandian, S. (2022). AMPK signaling in diabetes mellitus, insulin resistance and diabetic complications: A pre-clinical and clinical investigation. *Biomedicine & Pharmacotherapy, 146*, Article 112563. https://doi.org/10.1016/j.biopha.2021.112563

Faqerah, N., Walker, D., & Gerasimidis, K. (2023). The complex interplay between diet and Escherichia coli in inflammatory bowel disease. *Alimentary Pharmacology & Therapeutics, 58*(10), 984–1004. https://doi.org/10.1111/apt.17720

Feng, M., Liu, F., Xing, J., Zhong, Y., & Zhou, X. (2021). Anemarrhena saponins attenuate insulin resistance in rats with high-fat diet-induced obesity via the IRS-1/PI3K/AKT pathway. *Journal of Ethnopharmacology, 277*, Article 114251. https://doi.org/10.1016/j.jep.2021.114251

Fu, Q., Huang, H., Ding, A., Yu, Z., Huang, Y., Fu, G., Huang, Y., & Huang, X. (2022). *Portulaca oleracea* polysaccharides reduce serum lipid levels in aging rats by modulating intestinal microbiota and metabolites. *Frontiers. Nutrition, 9*. https://doi.org/10.3389/fnut.2022.965653

Fu, Y., Zhang, J., Chen, K., Xiao, C., Fan, L., Zhang, B., Ren, J., & Fang, B. (2019). An *in vitro* fermentation study on the effects of *Dendrobium officinale* polysaccharides on human intestinal microbiota from fecal microbiota transplantation donors. *Journal of Functional Foods, 53*, 44–53. https://doi.org/10.1016/j.jff.2018.12.005

Gao, K.-X., Peng, X., Wang, J.-Y., Wang, Y., Pei, K., Meng, X.-L., Zhang, S.-S., Hu, M.-B., & Liu, Y.-J. (2024). In vivo absorption, in vitro simulated digestion and fecal fermentation properties of polysaccharides from Pinelliae Rhizoma Praeparatum cum Alumine and their effects on human gut microbiota. *International Journal of Biological Macromolecules, 266*(2). https://doi.org/10.1016/j.ijbiomac.2024.131391. Article 131391.

Geng, X., Guo, D., Bau, T., Lei, J., Xu, L., Cheng, Y., Feng, C., Meng, J., & Chang, M. (2023). Effects of in vitro digestion and fecal fermentation on physico-chemical properties and metabolic behavior of polysaccharides from Clitocybe squamulosa. *Food Chemistry, X, 18, Article 100644*. https://doi.org/10.1016/j.fochx.2023.100644

Guo, W., Yun, J., Wang, B., Xu, S., Ye, C., Wang, X., Qu, Y., Zhao, F., & Yao, L. (2024). Comparative study on physicochemical properties and hypoglycemic activities of intracellular and extracellular polysaccharides from submerged fermentation of Morchella esculenta. *International Journal of Biological Macromolecules, 278*(Pt 2), 134759. https://doi.org/10.1016/j.ijbiomac.2024.134759

Han, R., Pang, D., Wen, L., You, L., Huang, R., & Kulikouskaya, V. (2020). *In vitro* digestibility and prebiotic activities of a sulfated polysaccharide from *Gracilaria Lemaneiformis*. *Journal of Functional Foods, 64, Article 103652*. https://doi.org/10.1016/j.jff.2019.103652

Han, X., Zhou, Q., Gao, Z., Lin, X., Zhou, K., Cheng, X., Chitrakar, B., Chen, H., & Zhao, W. (2022). *In vitro* digestion and fecal fermentation behaviors of polysaccharides from *Ziziphus Jujuba cv. Pozao* and its interaction with human gut microbiota. *Food Research International, 162, Article 112022*. https://doi.org/10.1016/j.foodres.2022.112022

Hu, W., Di, Q., Liang, T., Zhou, N., Chen, H., Zeng, Z., Luo, Y., & Shaker, M. (2023). Effects of *in vitro* simulated digestion and fecal fermentation of polysaccharides from straw mushroom (*Volvariella volvacea*) on its physicochemical properties and human gut microbiota. *International Journal of Biological Macromolecules, 239*. https://doi.org/10.1016/j.ijbiomac.2023.124188

Ji, Y., Su, A., Ma, G., Tao, T., Fang, D., Zhao, L., & Hu, Q. (2020). Comparison of bioactive constituents and effects on gut microbiota by *in vitro* fermentation between *Ophicordyceps sinensis* and *Cordyceps militaris*. *Journal of Functional Foods, 68*. https://doi.org/10.1016/j.jff.2020.103901

Kasipandi, M., Manikandan, A., Sreeja, P. S., Suman, T., Saikumar, S., Dhivya, S., & Parimelazhagan, T. (2019). Effects of *in vitro* simulated gastrointestinal digestion on the antioxidant, α-glucosidase and α-amylase inhibitory activities of water-soluble polysaccharides from *Opilia amentacea* roxb fruit. *Lwt-Food Science and Technology, 111*, 774–781. https://doi.org/10.1016/j.lwt.2019.05.079

Khalid, M., Alkaabi, J., Khan, M. A. B., & Adem, A. (2021). Insulin signal transduction perturbations in insulin resistance. *International Journal of Molecular Sciences, 22*(16). https://doi.org/10.3390/ijms22168590

Li, J., Ding, X., Jian, T., Lu, H., Zhao, L., Li, J., Liu, Y., Ren, B., & Chen, J. (2020). Four sesquiterpene glycosides from loquat (*Eriobotrya japonica*) leaf ameliorates palmitic acid-induced insulin resistance and lipid accumulation in HepG2 cells via AMPK signaling pathway. *Peerj, 8*, 10413. https://doi.org/10.7717/peerj.10413

Li, S., Li, M., Yue, H., Zhou, L., Huang, L., Du, Z., & Ding, K. (2018). Structural elucidation of a pectic polysaccharide from *Fructus Mori* and its bioactivity on intestinal bacteria strains. *Carbohydrate Polymers, 186*, 168–175. https://doi.org/10.1016/j.carbpol.2018.01.026

Li, W., Wang, C., Yuan, G., Pan, Y., & Chen, H. (2018). Physicochemical characterisation and α-amylase inhibitory activity of tea polysaccharides under simulated salivary, gastric and intestinal conditions. *International Journal of Food Science & Technology, 53*(2), 423–429. https://doi.org/10.1111/ijfs.13600

Liu, C., Zhang, J., Li, M., Zhao, L., Ji, C., & Ma, Q. (2018). Alterations and structural resilience of the gut microbiota under dietary fat perturbations. *Journal of Nutritional Biochemistry, 61*, 91–100. https://doi.org/10.1016/j.jnutbio.2018.07.005

Liu, N., Chen, M., Song, J., Zhao, Y., Gong, P., & Chen, X. (2022). Effects of *Auricularia auricula* polysaccharides on gut microbiota composition in type 2 diabetic mice. *Molecules, 27*(18), 6061. https://doi.org/10.3390/molecules27186061

Liu, Y., Li, Y., Zhang, W., Sun, M., & Zhang, Z. (2019). Hypoglycemic effect of inulin combined with ganoderma lucidum polysaccharides in T2DM rats. *Journal of Functional Foods, 55*, 381–390. https://doi.org/10.1016/j.jff.2019.02.036

Liu, Y., Wang, C., Li, J., Li, T., Zhang, Y., Liang, Y., & Mei, Y. (2020). *Phellinus linteus* polysaccharide extract improves insulin resistance by regulating gut microbiota composition. *FASEB Journal, 34*(1), 1065–1078. https://doi.org/10.1096/fj.201901943RR

Liu, Z., Wang, M., Meng, L., Chen, Y., Wang, Q., Zhang, Y., Xi, X., & Kang, W. (2023). Lignans from *Patrinia scabiosaefolia* improve insulin resistance by activating PI-3K/AKT pathway and promoting GLUT4 expression. *Food Science and Human Wellness, 12*(6), 2014–2021. https://doi.org/10.1016/j.fshw.2023.03.015

Liu, Z., Xu, L., Xing, M., Xu, X., Wei, J., Wang, J., & Kang, W. (2020). Trelagliptin succinate: DPP-4 inhibitor to improve insulin resistance in adipocytes. *Biomedicine & Pharmacotherapy, 125, Article 109952*. https://doi.org/10.1016/j.biopha.2020.109952

Ma, G., Du, H., Hu, Q., Yang, W., Pei, F., & Xiao, H. (2022). Health benefits of edible mushroom polysaccharides and associated gut microbiota regulation. *Critical Reviews in Food Science and Nutrition, 62*(24), 6646–6663. https://doi.org/10.1080/10408398.2021.1903385

Ma, G., Xu, Q., Du, H., Kimatu, B. M., Su, A., Yang, W., … Xiao, H. (2022). Characterization of polysaccharide from *Pleurotus eryngii* during simulated gastrointestinal digestion and fermentation. *Food Chemistry, 370, Article 131303*. https://doi.org/10.1016/j.foodchem.2021.131303

Ma, Q., Li, Y., Li, P., Wang, M., Wang, J., Tang, Z., Wang, T., Luo, L., Wang, C., & Zhao, B. (2019). Research progress in the relationship between type 2 diabetes mellitus and intestinal flora. *Biomedicine & Pharmacotherapy, 117, Article 109138*. https://doi.org/10.1016/j.biopha.2019.109138

McNabney, S. M., & Henagan, T. M. (2017). Short chain fatty acids in the Colon and Peripheral tissues: A focus on butyrate, Colon Cancer. *Obesity and Insulin Resistance. Nutrients, 9*(12), 1348. https://doi.org/10.3390/nu9121348

Niu, X., Lu, P., Huang, L., Sun, Y., Jin, M., Liu, J., & Li, X. (2024). The effect of metformin combined with liraglutide on gut microbiota of Chinese patients with type 2 diabetes. *International Microbiology, 27*(1), 265–276. https://doi.org/10.1007/s10123-023-00380-y

Nolan, C. J., Ruderman, N. B., Kahn, S. E., Pedersen, O., & Prentki, M. (2015). Insulin resistance as a physiological defense against metabolic stress: Implications for the Management of Subsets of type 2 diabetes. *Diabetes, 64*(3), 673–686. https://doi.org/10.2337/db14-0694

Park, C. H., Han, D. S., Oh, Y.-H., Lee, A. R., Lee, Y.-R., & Eun, C. S. (2016). Role of *Fusobacteria* in the serrated pathway of colorectal carcinogenesis. *Scientific Reports, 6, Article 25271*. https://doi.org/10.1038/srep25271

Porter, N. T., & Martens, E. C. (2017). The critical roles of polysaccharides in gut microbial ecology and physiology. In S. Gottesman (Ed.), *Vol: Vol. 71. Annual review of microbiology, Vol 71* (pp. 349–369).

Ren, B., Chen, C., Li, C., Fu, X., You, L., & Liu, R. H. (2017). Optimization of microwave-assisted extraction of *Sargassum thunbergii* polysaccharides and its antioxidant and hypoglycemic activities. *Carbohydrate Polymers, 173*, 192–201. https://doi.org/10.1016/j.carbpol.2017.05.094

Ren, R., Gao, X., Shi, Y., Li, J., Peng, L., Sun, G., Wang, Z., Yan, B., Zhi, J., & Yang, Y. (2021). Long-term efficacy of low-intensity single donor fecal microbiota transplantation in ulcerative colitis and outcome-specific gut Bacteria. *Frontiers in Microbiology, 12, Article 742255*. https://doi.org/10.3389/fmicb.2021.742255

Saad, M. J. A., Santos, A., & Prada, P. O. (2016). Linking gut microbiota and inflammation to obesity and insulin resistance. *Physiology, 31*(4), 283–293. https://doi.org/10.1152/physiol.00041.2015

Su, J., Tang, L., Luo, Y., Xu, J., & Ouyang, S. (2023). Research progress on drugs for diabetes based on insulin receptor/insulin receptor substrate. *Biochemical Pharmacology, Article, 115830*. https://doi.org/10.1016/j.bcp.2023.115830

Sun, J., Wu, K., Wang, P., Wang, Y., Wang, D., Zhao, W., Zhao, Y., Zhang, C., & Zhao, X. (2024). Dietary tomato pectin attenuates hepatic insulin resistance and inflammation in high-fat-diet mice by regulating the PI3K/AKT pathway. *Foods, 13*(3). https://doi.org/10.3390/foods13030444

Sun, Y., Hu, J., Zhang, S., He, H., Nie, Q., Zhang, Y., Chen, C., Geng, F., & Nie, S. (2021). Prebiotic characteristics of arabinogalactans during in vitro fermentation through multi-omics analysis. *Food and Chemical Toxicology, 156, Article 112522*. https://doi.org/10.1016/j.fct.2021.112522

Tian, J., Wang, X., Zhang, X., Chen, X., Dong, M., Rui, X., Zhang, Q., Jiang, M., & Li, W. (2023a). Artificial simulated saliva, gastric and intestinal digestion and fermentation in vitro by human gut microbiota of intrapolysaccharide from Paecilomyces cicadae TJJ1213. *Food Science and Human Wellness, 12*(2), 622–633. https://doi.org/10.1016/j.fshw.2022.07.065

Tian, J., Wang, X., Zhang, X., Chen, X., Dong, M., Rui, X., Zhang, Q., Jiang, M., & Li, W. (2023b). Artificial simulated saliva, gastric and intestinal digestion and fermentation *in vitro* by human gut microbiota of intrapolysaccharide from *Paecilomyces cicadae* TJJ1213. *Food Science and Human Wellness, 12*(2), 622–633. https://doi.org/10.1016/j.fshw.2022.07.065

Wang, C., Li, W., Chen, Z., Gao, X., Yuan, G., Pan, Y., & Chen, H. (2018). Effects of simulated gastrointestinal digestion *in vitro* on the chemical properties, antioxidant activity, α-amylase and α-glucosidase inhibitory activity of polysaccharides from *Inonotus obliquus*. *Food Research International, 103*, 280–288. https://doi.org/10.1016/j.foodres.2017.10.058

Wang, J., Wang, C., Li, S., Li, W., Yuan, G., Pan, Y., & Chen, H. (2017). Anti-diabetic effects of *Inonotus obliquus* polysaccharides in streptozotocin-induced type 2 diabetic mice and potential mechanism via PI3K-Akt signal pathway. *Biomedicine & Pharmacotherapy, 95*, 1669–1677. https://doi.org/10.1016/j.biopha.2017.09.104

Wang, L., Zhang, P., Li, C., Xu, F., & Chen, J. (2022). A polysaccharide from *Rosa roxburghii* Tratt fruit attenuates high-fat diet-induced intestinal barrier dysfunction and inflammation in mice by modulating the gut microbiota. *Food & Function, 13*(2), 530–547. https://doi.org/10.1039/d1fo03190b

Wang, Q., Wang, F., Xu, Z., & Ding, Z. (2017). Bioactive mushroom polysaccharides: A review on monosaccharide composition, biosynthesis and regulation. *Molecules, 22 (6), Article 955*. https://doi.org/10.3390/molecules22060955

Wang, Y., Chen, G., Peng, Y., Rui, Y., Zeng, X., & Ye, H. (2019). Simulated digestion and fermentation *in vitro* with human gut microbiota of polysaccharides from *coralline pilulifera*. *Lwt-Food Science and Technology, 100*, 167–174. https://doi.org/10.1016/j.lwt.2018.10.028

Wardman, J. F., Bains, R. K., Rahfeld, P., & Withers, S. G. (2022). Carbohydrate-active enzymes (CAZymes) in the gut microbiome. *Nature Reviews Microbiology, 20*(9), 542–556. https://doi.org/10.1038/s41579-022-00712-1

Wu, H., Chen, J., Liu, Y., Cheng, H., Nan, J., Park, H. J., … Li, J. (2023). Digestion profile, antioxidant, and antidiabetic capacity of *Morchella esculenta* exopolysaccharide: *In vitro*, *in vivo* and microbiota analysis. *Journal of the Science of Food and Agriculture, 103*(9), 4401–4412. https://doi.org/10.1002/jsfa.12513

Wu, J., Lin, Z., Wang, X., Zhao, Y., Zhao, J., Liu, H., … Ma, X. (2022). Limosilactobacillus reuteri SLZX19-12 protects the Colon from infection by enhancing stability of the gut microbiota and barrier integrity and reducing inflammation. *Microbiology Spectrum, 10*(3). https://doi.org/10.1128/spectrum.02124-21

Xiang, H., Sun-Waterhouse, D., & Cui, C. (2021). Hypoglycemic polysaccharides from *Auricularia auricula* and *Auricularia polytricha* inhibit oxidative stress, NF-κB signaling and proinflammatory cytokine production in streptozotocin-induced diabetic mice. *Food Science and Human Wellness, 10*(1), 87–93. https://doi.org/10.1016/j.fshw.2020.06.001

Xiao, X., Sun, Q., Kim, Y., Yang, S.-H., Qi, W., Kim, D., … Park, Y. (2018). Exposure to permethrin promotes high fat diet-induced weight gain and insulin resistance in male C57BL/6J mice. *Food and Chemical Toxicology, 111*, 405–416. https://doi.org/10.1016/j.fct.2017.11.047

Xie, F., Zou, T., Chen, J., Liang, P., Wang, Z., & You, J. (2022). Polysaccharides from *Enteromorpha prolifera* improves insulin sensitivity and promotes adipose thermogenesis in diet-induced obese mice associated with activation of PGC-1α-FNDC5/irisin pathway. *Journal of Functional Foods, 90*. https://doi.org/10.1016/j.jff.2022.104994

Xu, B., Song, S., Yao, L., Wang, H., Sun, M., Zhuang, H., Zhang, X., Liu, Q., Yu, C., & Feng, T. (2024). Digestion under saliva, simulated gastric and small intestinal conditions and fermentation in vitro by human gut microbiota of polysaccharides from Ficus carica Linn. *Food Hydrocolloids, 146, Article 109204*. https://doi.org/10.1016/j.foodhyd.2023.109204

Xu, L., Li, Y., Dai, Y., & Peng, J. (2018). Natural products for the treatment of type 2 diabetes mellitus: Pharmacology and mechanisms. *Pharmacological Research, 130*, 451–465. https://doi.org/10.1016/j.phrs.2018.01.015

Yu, R., Luo, J., Liu, L., & Peng, X. (2023). Hypoglycemic effect of edible Fungi polysaccharides depends on their metabolites from the fermentation of human fecal microbiota. *Foods, 13(1), Article 97*. https://doi.org/10.3390/foods13010097

Yuan, Q., He, Y., Xiang, P.-Y., Huang, Y.-J., Cao, Z.-W., Shen, S.-W., Zhao, L., Zhang, Q., Qin, W., & Wu, D.-T. (2020). Influences of different drying methods on the structural characteristics and multiple bioactivities of polysaccharides from okra (*Abelmoschus esculentus*). *International Journal of Biological Macromolecules, 147*, 1053–1063. https://doi.org/10.1016/j.ijbiomac.2019.10.073

Zhang, J., Wang, S., Zeng, Z., Qin, Y., Shen, Q., & Li, P. (2020). Anti-diabetic effects of *Bifidobacterium animalis* 01 through improving hepatic insulin sensitivity in type 2 diabetic rat model. *Journal of Functional Foods, 67, Article 103843*. https://doi.org/10.1016/j.jff.2020.103843

Zhang, Y., Wang, D., Chen, Y., Liu, T., Zhang, S., Fan, H., Liu, H., & Li, Y. (2021). Healthy function and high valued utilization of edible fungi. *Food Science and Human Wellness, 10*(4), 408–420. https://doi.org/10.1016/j.fshw.2021.04.003

Zhang, Z., Sun, L., Chen, R., Li, Q., Lai, X., Wen, S., Cao, J., Lai, Z., Li, Z., & Sun, S. (2024). Recent insights into the physicochemical properties, bioactivities and their

relationship of tea polysaccharides. *Food Chemistry, 432*. https://doi.org/10.1016/j.foodchem.2023.137223

Zhao, X., An, X., Yang, C., Sun, W., Ji, H., & Lian, F. (2023). The crucial role and mechanism of insulin resistance in metabolic disease. *Frontiers in Endocrinology, 14, Article 1149239*. https://doi.org/10.3389/fendo.2023.1149239

Zhou, Y.-J., Xu, N., Zhang, X.-C., Zhu, Y.-Y., Liu, S.-W., & Chang, Y.-N. (2021). Chrysin improves glucose and lipid metabolism disorders by regulating the AMPK/PI3K/AKT signaling pathway in insulin-resistant HepG2 cells and HFD/STZ-induced C57BL/6J mice. *Journal of Agricultural and Food Chemistry, 69*(20), 5618–5627. https://doi.org/10.1021/acs.jafc.1c01109